International Journal on
"Technical and Physical Problems of Engineering"
(IJTPE)
Published by International Organization of IOTPE

ISSN 2077-3528
IJTPE Journal
www.iotpe.com
ijtpe@iotpe.com

June 2022 | Issue 51 | Volume 14 | Number 2 | Pages 360-368

STUDY OF EFFECT OF MATERIAL PARAMETERS ON SPRING BACK OF HYDROFORMED PARTS

Y. Fartouh [1,2] Y. Dahbi [1,2] M. Nassraoui [2] O. Bouksour [2]

1. National Higher School of Electricity and Mechanics, ENSEM, Hassan II University, Oasis, Casablanca, Morocco
yassine.fartouh-etu@etu.univh2c.ma, youssef.dahbi-etu@etu.univh2c.ma
2.Laboratory of Mechanics, Production and Industrial Engineering, LMPGI, Higher School of Technology of Casablanca, ESTC, Hassan II University, Oasis, Casablanca, Morocco
mohammed.nassraoui@univh2c.ma, otmane.bouksour@univh2c.ma

Abstract- Spring back is one of the most common problems in the sheet metal forming operation now a day (for example stamping, hydroforming, bending, etc.) [1]. The Spring back is a geometric phenomenon that affects accuracy by changing the geometric shape. The most prominent feature of sheet metal forming process is an elastic recovery phenomenon during unloading which leads to spring. In this paper, we present a mathematical model to study the hydroforming process of the sheets, and exploit the numerical simulation by the finite element method (FEM) to identify the Spring back of the deformed sheet, and study the effect of different material parameters: work hardening "*n*" and anisotropy parameters "*K*" on the spring back of the hydroformed parts. The results obtained show the influence of these parameters on the spring back. Moreover, materials with high strain hardening coefficients are always desired to obtain the maximum deformation, which allows to reduce the spring back.

Keywords: Hydroforming, Numerical Simulation, Finite Element, Spring Back.

1. INTRODUCTION

Hydroforming is a recent process that shows several advantages several advantages over conventional processes. This technology is widely used to obtain complex shaped parts in a single operation. Hydroforming consists of plastically deforming sheets or tubes in a die using the driving force of a fluid (water, hydraulic oil, emulsion) under pressure which, injected inside a tube or only one side of the sheet insert inside a stamp or mold, in order to manufacture metal parts of complex shape as Figure 1 [2].

Hydroforming is widely applied in manufacturing due to the increasing demand for lightweight parts in sectors such as the automotive, aerospace and naval industries [3, 4]. Compared to conventional stamping and welding, hydroforming offers several advantages, such as: high lightness of the manufactured part; low tooling and assembly costs; good rigidity and mechanical strength; reduction in the number of components needed to make an assembly; good geometric accuracy and a considerable reduction in material losses. The hydroforming process still requires good control of its parameters in order to manufacture parts with suitable specifications. One method of determining the parameters for this process is the study and analysis of hydraulic swelling test [3, 5, 6].

The realization of experiments and numerical simulations (FEM) is a significant help for the success of this process. Indeed, complex processes can be realized virtually, which contributes significantly to their mastery. In this study we propose to investigate by numerical analysis (FEM) the influence of work hardening and anisotropy parameters on the hydroforming of thin sheets and especially on the spring back after load removal.

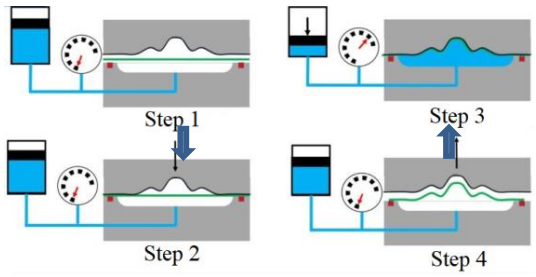

Figure 1. Principle of the sheet hydroforming process

Figure 2. Examples of hydroformed parts [7]

2. SHEET HYDROFORMING MODELLING

Most sheet metal forming processes (stamping, etc.) use an elasto-plastic approach to study the behavior of sheets. The elasto-plastic theory comprises two different approaches, each describing a physical scale of behavior (the phenomenological approach and the microscopic approach). Both approaches allow to describe the evolution of the state of stress and strain during a succession of deformations [8].

The elastoplastic behavior of the material is described by an envelope called the initial load surface defined in the stress space. This closed surface marks the elastic limit and the beginning of the plastic flow of the material for the different possible loading configurations, it is a generalization of the uniaxial elastic limit. We then introduce the notion of the plasticity criterion which can be isotropic (von Mises, Tresca, …) or anisotropic such as the Hill criteria 48, [9] which allows to describe the general anisotropy as well as the orthotropic anisotropy specific to sheets.

After defining the shape of the loading surfaces through the plasticity criteria, these surfaces change in size throughout the loading process. However, throughout the loading process, these surfaces change in size: this is plastic strain hardening. When the shape of the surface is kept unchanged and only its size changes, the work hardening is said to be isotropic and described by a work hardening curve [3]. The tensile test along the rolling direction is often chosen as the reference test to establish the strain hardening curve relating the evolution of the elastic limit to the internal strain hardening variable. These curves are approximated by analytical functions which can take several forms. We consider Swift's hardening law or Hollomon's law:

Hollomon's work hardening law:

$$\bar{\sigma} = k\bar{\varepsilon}^{n} \tag{1}$$

Swift's work hardening law:

$$\bar{\sigma} = k\left(\varepsilon_0 + \varepsilon\right)^{n} \tag{2}$$

2.1. Analytic Solution

In the present paper, a mathematical model is presented to exploit the circular expansion test while adopting a Hill48 anisotropic plasticity criteria for the description of the sheet behavior. Assuming that the principal stress frame coincides with the orthotropic frame and with the assumption of plane stresses, an expression for the Hill48 criteria is made explicit. The equivalent stress in the principal frame is defined by [3]:

$$\bar{\sigma} = \frac{\sqrt{r_{90}\left(1+r_0\right) - 2r_0 r_{90}\Omega + r_0\left(1+r_{90}\right)\Omega^2}}{\sqrt{r_{90}\left(1+r_0\right)}}\sigma_1 \tag{3}$$

where, Ω is defined by:

$$\Omega = \frac{\sigma_2}{\sigma_1} \tag{4}$$

Considering an associated flow law, the equivalent deformation is written:

$$d\bar{\varepsilon} = \frac{\sqrt{1+r_0\sqrt{r_0\left(1+r_{90}\right)+2r_0 r_{90}\beta + r_{90}\left(1+r_0\right)\beta^2}}}{\sqrt{r_0 + r_0 r_{90} + r_0{}^2}}d\varepsilon_1 \tag{5}$$

where, β is defined by, Equation (6):

$$\beta = \frac{d\varepsilon_2{}^{p}}{d\varepsilon_1{}^{p}} \tag{6}$$

The stress ratio is related to the strain ratio by the relationship, Equation (7) [3]:

$$\beta = \frac{r_0\left(1+r_{90}\right)\Omega - r_0 r_{90}}{r_{90}\left(1+r_0\right) - r_0 r_{90}\Omega} \tag{7}$$

In the orthotropic material frame the stress state at the pole of a swollen sheet is defined by the stress tensor, Equation (8):

$$\sigma = \begin{bmatrix} \sigma_1 & 0 & 0 \\ 0 & \sigma_2 & 0 \\ 0 & 0 & 0 \end{bmatrix} \tag{8}$$

The principal stresses are assumed to coincide with the orthotropy axes, which implies that the coaxially condition is satisfied. It follows that the strain tensor is also diagonal in the orthotropic reference frame and is written:

$$\varepsilon = \begin{pmatrix} \varepsilon_1 & 0 & 0 \\ 0 & \varepsilon_2 & 0 \\ 0 & 0 & \varepsilon_3 \end{pmatrix} \tag{9}$$

The equilibrium equation (Pascal's equation) is defined by, equation (10):

$$\frac{\sigma_1}{R_\theta} + \frac{\sigma_2}{R_\varphi} = \frac{P}{e} \tag{10}$$

where, σ_1, σ_2 are the principal stresses (coincident with the orthotropy axes), R_θ and R_φ are the radius of curvature along the two principal directions, respectively, P the inflation pressure and e the current thickness at the pole of the sheet (Figures 3 and 4).

By introducing the stress ratio Ω and assuming that $R_\theta \approx R_\varphi = \rho$, the equilibrium equation reduces to:

$$\sigma_1 = \frac{P\rho}{\left(1+\Omega\right)e} \tag{11}$$

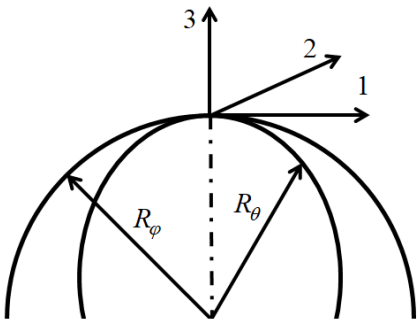

Figure 3. Setting up a circular expansion test: test elements, [3], [5]

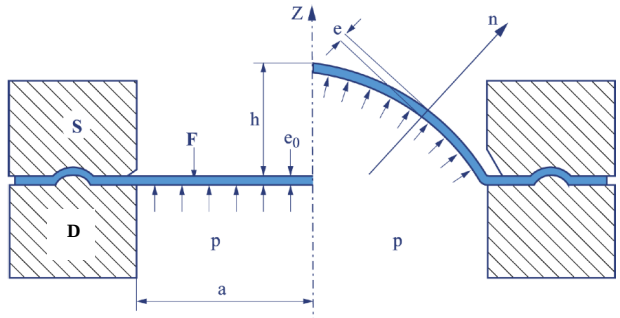

Before test After test
F =Flanc S = Serre-flanc D =Die

Figure 4. Setting up a circular expansion test: Geometry of the sheet deformed [3], [5]

Assuming that the geometry of the deformed sheet is spherical, the radius of curvature ρ can be deduced from the height of the dome h over a radius an according to the relation of the spherometer [9].

$$\rho = \frac{a^2 + h^2}{2h} \tag{12}$$

It can be demonstrated that the principal strain is defined by:

$$\varepsilon_1 = \ln\left(1 + \frac{h^2}{a^2}\right) \tag{13}$$

So far, the principal stress and strain are known as a function of the measurable variables (h, a, e, P). In order to establish a direct relationship between forces and strains, it remains to determine the ratio Ω. To do so, *a* state of normal anisotropy will be assumed as a first approximation. This reduced the number of anisotropy parameters to the single parameter $\bar{r}$. In this case, the behavior is isotropic in the plane of the sheet, resulting in an equi-biaxial stress and strain state ($\beta = \Omega = 1$). The equivalent stress and strain are then defined by, Equations (14) and (15):

$$\bar{\sigma} = \sqrt{\frac{2}{(1+r)}}\sigma_1 \tag{14}$$

$$d\bar{\varepsilon} = \sqrt{2(1+\bar{r})}\, d\bar{\varepsilon}_1 \tag{15}$$

Using a Hollomon type strain hardening law (1) combined with Equations (3) and (5) and taking into account the equivalent strain expression, the equivalent stress is then defined by, Equation (16):

$$\bar{\sigma} = k\left(\sqrt{2(1+\bar{r})}\ln\left(1 + \frac{h^2}{a^2}\right)\right)^n \tag{16}$$

Based on the assumption of plastic incompressibility, the current thickness at the pole is defined from the initial thickness e_0 by:

$$e = e_0 \exp\left(2\ln\left(1 + \frac{h^2}{a^2}\right)\right) \tag{17}$$

The final equation relating expansion pressure to dome height is deduced from Equations (12), (16), (17) and taking into account the expression of the equivalent stress:

$$P = 2\sqrt{2(1+\bar{r})}\, k \frac{e_0 h}{a^2} \frac{1}{\left(1 + \frac{h^2}{a^2}\right)^3}\left(\sqrt{2(1+\bar{r})}\ln\left(1 + \frac{h^2}{a^2}\right)\right)^n \tag{18}$$

2.1. Numerical Application

To quantify the value of the height at the pole as a function of the pressure applied to the sheet using the Equation (18), the values listed in Table 1 are taken [6]:

Table 1. Theoretical calculation data

Coefficient of anisotropy	$\bar{r} = 1.68$
Radius of the sheet	a = 102.15 mm
Modulus of hardening	K = 536 MPa
Hardening coefficient	n = 2.24
Fluid pressure	P = 2.061 MPa

Using Equation (18), we find a height of the pole:

$$h \approx 17.6\,\text{mm} \tag{19}$$

The height at the pole h obtained by theoretical calculation taking into account the values quoted in Table 1, is similar to the results obtained by numerical simulation presented in section 3.

3. NUMERICAL SIMULATION

The finite element method is used to explore the influence of strain hardening and anisotropy on the response of a thin circular sheet. To do this, we built a three-dimensional (3D) model with 8777 nodes and 17230 S3R elements, using ABAQUS software, which is used to take into account the non-linearities of the hydroforming process (contact between the sheet and the die, ...).

3.1. Digital Modelling of the Sheet Metal Hydroforming Process

To model the hydroforming test of the sheet (circular swelling test) we used the "PART" module of the ABAQUS CAE software. The sheet was represented in 3D mode (deformable shell type), while the matrix was represented in rigid solid mode (unreformable), which allows to reduce the calculation time. The two sub-assemblies are then used for the development of the 3D model (Figure 5 and Table 2).

Table 2. Geometrical characteristics of the sheet and the die

Diameter of the sheet	204.3 mm
Thickness of the sheet	2 mm
Diameter of the die	198

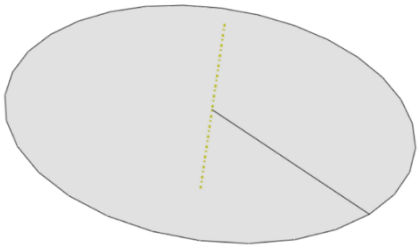

(a) Sheet metal

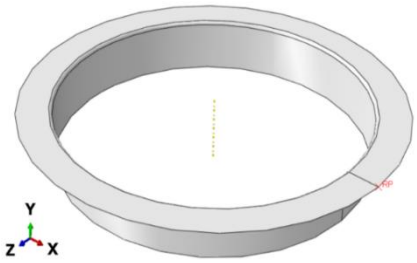

(b) Die

Figure 5. Two parts of the model, (a) sheet metal, (b) the die

3.2. Material Properties

Before proceeding to the ABAQUS assembly stage, we created the material properties associated only with the deformable part (here the sheet metal). The material chosen here is (S235) which is characterized by the following properties:
Young's modulus: 210000 MPa
Poisson's ratio: 0.3
Density: 7850 Kg/m^3
and the data related to the plastic field as Table 3.

Table 3. Plastic properties (stresses, strains)

Stress (MPa)	Plastic strains (mm)
235	0
238.153859922664	0.00344369650676006
241.96155275114	0.00389327344220596
245.769245579617	0.00441475761752347
249.576938408094	0.0050187331596658
253.384631236571	0.00571714263467511
257.192324065047	0.00652343661516063
261.000016893524	0.0074527370723376
264.807709722001	0.00852201563367118
268.615402550478	0.00975028780827693
272.423095378954	0.0111588243459402
276.230788207431	0.0127713809620005
280.038481035908	0.0146144477294734
283.846173864385	0.0167175195117272
287.653866692862	0.0191133888838607
291.461559521338	0.0218384630687229
295.269252349815	0.0249331064943438
299.076945178292	0.0284420106634871
302.884638006769	0.0324145931131598
306.692330835246	0.0369054273323082
310.500023663722	0.0419747055996599
314.307716492199	0.0476887368008225
318.115409320676	0.0541204813844055
321.923102149152	0.0613501257211514
325.730794977629	0.0694656982379622
329.538487806106	0.0785637298103286
333.346180634583	0.0887499610121265
337.15387346306	0.100140098941102
340.961566291536	0.112860626461718
344.769259120013	0.127049666834466
348.57695194849	0.142857906832306
352.384644776967	0.160449581580779
356.192337605443	0.180003524498445
360.00003043392	0.201714285858934

3.1. Development of Numerical Model by ABAQUS

After the definition of the material, we created a shell section associated to the deformable part (the sheet). The thickness of 2 mm is defined for the sheet in this section we also defined the integration mode in order to evaluate the behavior of the material at each integration point, for a better accuracy and to reduce the calculation time we use the Gauss method. After the assembly of the model that constitutes the two parts (sheet and die), the mesh of the deformable part is made and the boundary conditions are defined as Figure 6.

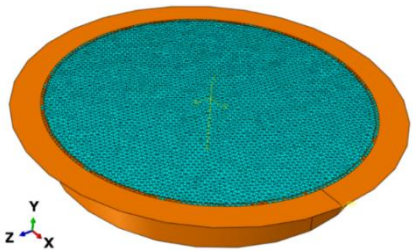

Figure 6. Mesh size of the sheet

To facilitate the deformation of the sheet as the pressure increases, and to model the actual hydroforming test of the sheets several steps are created. We used a linear pressure profile over time from an initial value of 0 MPa and a final value of 2 MPa. The sheet is expanded under this loading.

The hydroforming process is very sensitive to frictional forces, particularly with regard to crease formation, localization of thickness variations and tear defects [10]. The Coulomb method between two surfaces in contact can accept a certain degree of shear stress before they start to slide relative to each other. The Coulomb model defines a critical shear stress. This is calculated with the Equation (20):

$$\tau_{critique} = \mu \times P \tag{20}$$

where, P is the pressure of contact.

The friction model assumes that μ is the same in all directions. There are two orthogonal friction components, τ_1 and τ_2. ABAQUS assumes the two components exerted on the two contacting surfaces as an equivalent shear stress:

$$\bar{\tau} = \sqrt{{\tau_1}^2 + {\tau_2}^2} \tag{21}$$

4. RESULTS AND DISCUSSION

4.1. Influence of Anisotropy $\bar{r}$

Figure 7 shows the expansion pressure versus dome height curves for various anisotropy coefficients ($\bar{r} = 0.5$, $\bar{r} = 1$ and $\bar{r} = 2$) [3].

We note that: The expansion pressure increases gradually up to a maximum pressure, called the rupture pressure, after which it starts to decrease, although the sheet continues to expand, which causes a phase of deformation known as unstable.

The rupture pressure P_{max} is very sensitive to the coefficient of anisotropy ($\bar{r} = 0.5$, $\bar{r} = 1$ and $\bar{r} = 2$); P_{max} increases with $\bar{r}$. The model shows that the height the material reaches at failure pressure is independent of the anisotropy coefficient as Figure 7.

4.2 Influence of the Hardening Coefficient

To study the effect of the strain hardening coefficient, we varied this coefficient between 0.2 and 0.4. And for the work hardening modulus we used a value of K=500 MPa. Table 4 and Figures 8-10 illustrate the evolution of the displacement of the plate for the different values of the work hardening coefficient. We can see that the higher the coefficient n the greater the displacement.

The influence of the work hardening coefficient "n" on the spring back of the hydroformed sheet is also studied and we remark that the spring back is less important for higher values of n (n=0.4) as Figures 11-13 and Table 5.

Table 4. Maximum displacement as a function of the strain hardening coefficient n

Hardening coefficient	Maximal displacement in mm	
n=0.2	10.8 mm	Figure 8
n=0.3	14.6 mm	Figure 9
n=0.4	18.6 mm	Figure 10

Table 5. The spring back as a function of the coefficient n

Hardening coefficient	Spring back in %	
n=0.2	4.273%	Figure 10
n=0.3	1.355%	Figure 11
n=0.4	0.305%	Figure 12

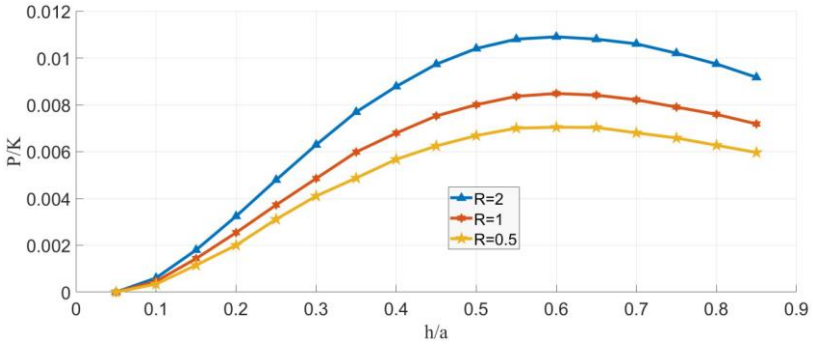

Figure 7. Height variation as a function of pressure and anisotropy coefficient [3]

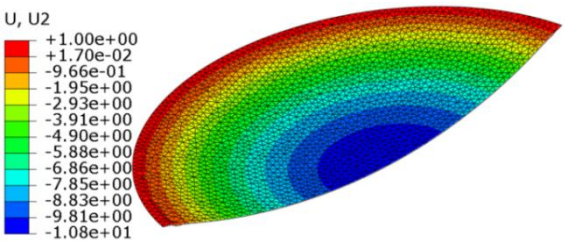

Figure 8. Displacement U2 of the sheet in mm for n=0.2

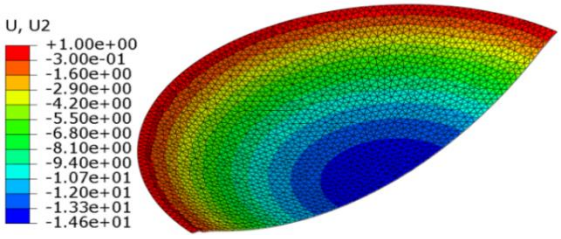

Figure 9. Displacement U2 of the sheet in mm for n=0.3

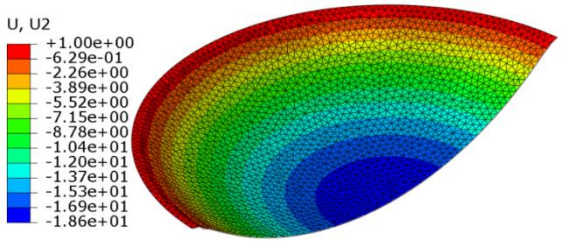

Figure 10. Displacement U2 of the sheet in mm for n=0.4

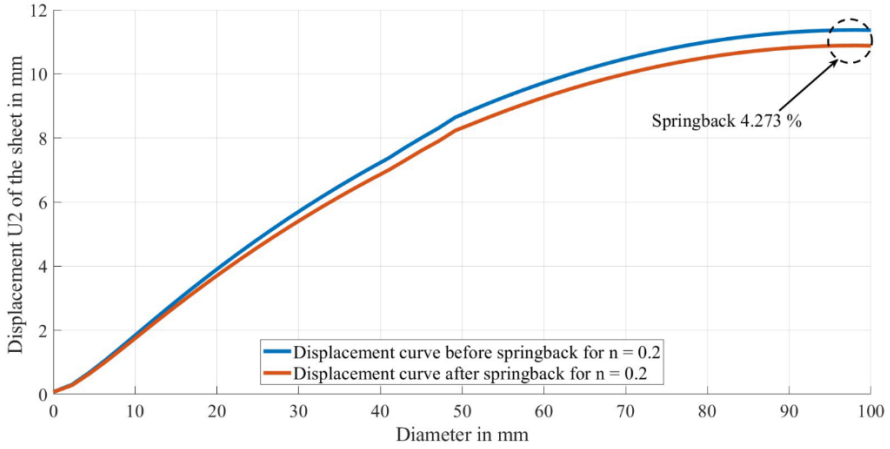

Figure 11. Displacement U2 of the sheet in mm for n=0.2

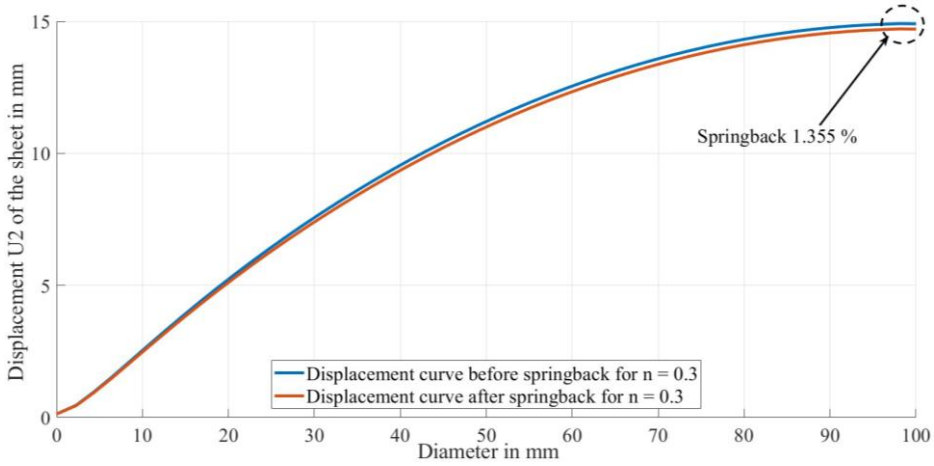

Figure 12. Displacement U2 of the sheet in mm for n=0.3

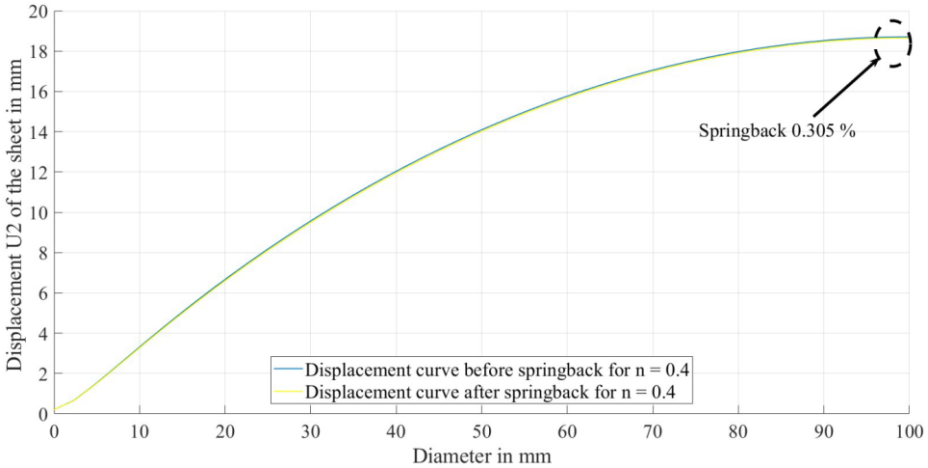

Figure 13. Displacement U2 of the sheet in mm for n=0.4

4.3. Influence of the Hardening Modulus

The effect of the coefficient K or the hardening modulus on the displacement of the deformed sheet is also studied. These numerical simulations are performed with the following parameters: n=0.3, and varying K between K=400 MPa and K=600 MPa. Figure 14 and Table 6 show that for the lowest work hardening modulus, the maximum displacement at the pole of the deformed sheet is the most important.

Table 6. Displacement at the pole as a function of the hardening modulus K

Hardening modulus (MPa)	Displacement at the pole (mm)
K=400	17.31
K=500	14.70
K=600	12.98

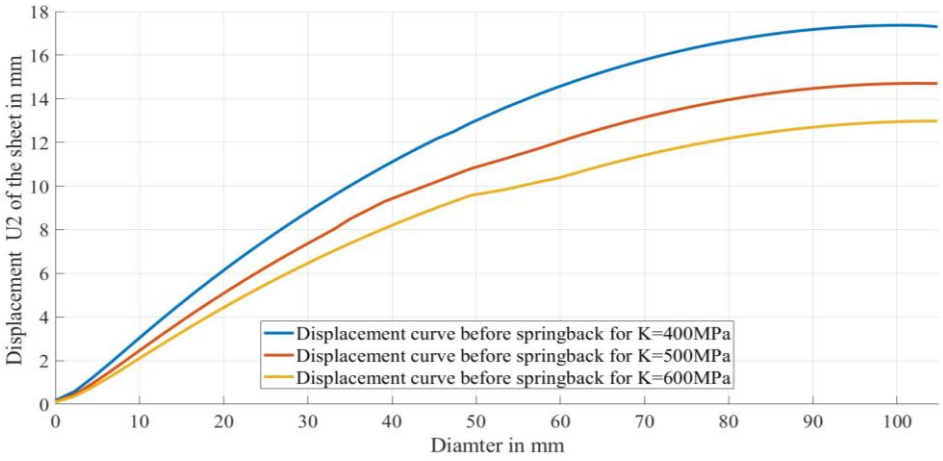

Figure 14. Displacement profile U2 of the sheet in mm for different values of *K*

We have studied the influence of the work hardening modulus *K* on the spring back of the hydroformed sheets, we remark that for the value of *K*=400 MPa the spring back is low compared to the results of the other hardening modulus (*K*=500 MPa and *K*=600 MPa) (Table 7 and Figures 15-17).

Table 7. The spring back as a function of the modulus *K*

Hardening modulus (MPa)	Spring back in %	
K=400	0.305 %	Figure 17
K=500	1.356 %	Figure 16
K=600	2.513 %	Figure 15

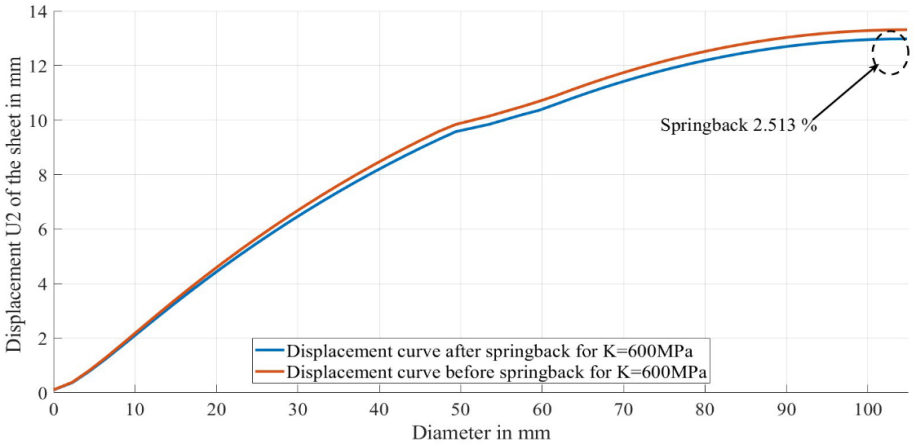

Figure 15. Displacement U2 of the sheet in mm for *K* =600 MPa

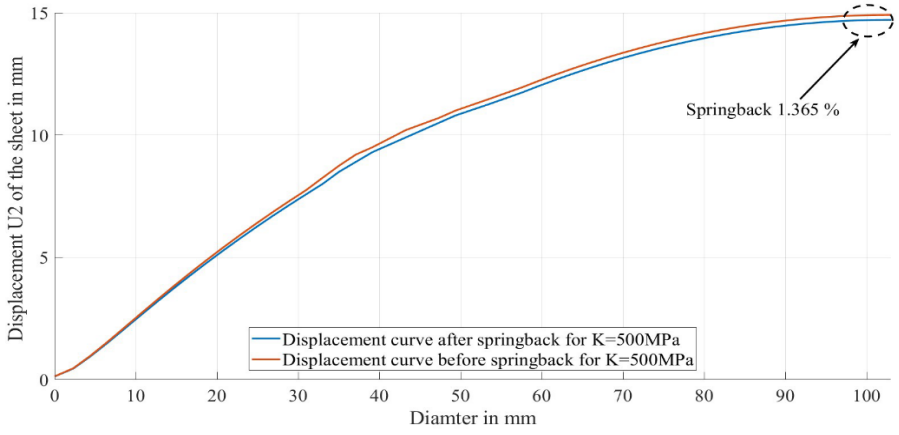

Figure 16. Displacement U2 of the sheet in mm for *K* =500 MPa

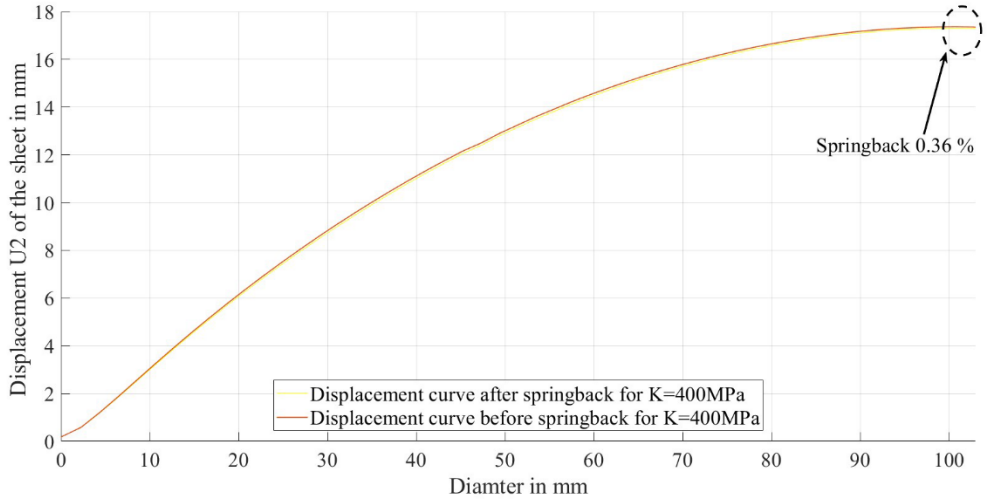

Figure 17. Displacement U2 of the sheet in mm for K =400 MPa

5. CONCLUSION

We presented a mathematical model to study the sheet hydroforming process based on the modelling of the circular expansion test. Also, we have exploited the numerical simulation by ABAQUS/explicit software to simulate the hydroforming process. This allows us to study and analyze the influence of each coefficient K, n and r on the sheet hydroforming process. We have also shown that there is a springbok at the end of the hydroforming process which is mainly due to stress relaxation after the removal of the load. The numerical results demonstrated the sensitivity of the process to material parameters. Moreover, materials with high strain hardening coefficients are always desired to obtain the maximum deformation, which allows to reduce the spring back.

REFERENCES

[1] F.E. Nouman, S.A. Nama, H.H. Mahdi, "Effect of Infill Percentage for 3D Printed Dies on Spring Back for Aluminum Sheets", International Journal on Technical and Physical Problems (IJTPE), Issue 49, Vol. 13, No. 4, pp. 27-32, December 2021.

[2] P. Hein, F. Vollertsen, "Hydroforming of Sheet Metal Pairs", Journal of Materials Processing Technology, Vol. 87, No. 1, pp. 154-164, March 1999.

[3] M. Ben Tahar, "Contribution to the Study and Simulation of the Hydroforming Process", Ph.D. Thesis, National School of Mines of Paris, 2005.

[4] N. Asnafi, T. Nilsson, G. Lassl, "Tubular Hydroforming of Automotive Side Members with Extruded Aluminum Profiles", Journal of Materials Processing Technology, Vol. 142, No. 1, pp. 93-101, November 2003.

[5] M. Nassraoui, B. Radi, "Modelling and Numerical Simulation of Hydroforming", Uncertainties and Reliability of Metaphysical Systems, Vol. 2, No. 1, pp. 26-40, May 2018.

[6] N. Mohammed, R. Bouchaib, "Study of Optimizing a Tube Hydroforming", The 4th IEEE International Colloquium on Information Science and Technology (CiSt), pp. 713-718, Tangier, Morocco, October 2016.

[7] A. Kocanda, H. Sadlowska, "Automotive Component Development by Means of Hydroforming", Archives of Civil and Mechanical Engineering, Vol. 8, No. 3, pp. 55-72, 2008.

[8] M.A. Ben Abdessalem, "Optimization with Taking into Account of Uncertainties in Hydroforming Process", No. ISAM0003, Rouen, France, June 2011, https://tel.archives-ouvertes.fr.

[9] R. Hill, "C.A Theory of the Plastic Bulging of a Metal Diaphragm by Lateral Pressure", London Edinburgh Dublin Philosophical Magazine Journal of Science, Vol. 41, Issue 322, pp. 1133-1142, January 1950.

[10] R.J. Boulbes, "Contact, in Troubleshooting Finite-Element Modeling with Abaqus: With Application in Structural Engineering Analysis", Springer International Publishing, pp. 227-295, 2020.

BIOGRAPHIES

Yassine Fartouh was born in El Jadida, Morocco, in 1989. He obtained his Master degree specialized in mechanical engineering from Higher Normal School of Technical Education (ENSET), University of Mohamed V (Rabat, Morocco) in 2014 and the degree of Aggregation in Industrial Engineering Sciences and Mechanical Engineering (Settat, Morocco) in 2019. Currently, he is a teacher at Preparatory Classes for the High Schools in Morocco, Ministry of National Education (Safi, Morocco). His research focuses on numerical modeling of structures.

Youssef Dahbi was born in Settat, Morocco, in 1991. He obtained his Master degree specialized in mechanical engineering from Faculty of Science and Technology, Fez (FSTF) USMBA - Sidi Mohamed Ben Abdellah University (Fez, Morocco). Currently, he is a teacher of engineering sciences in Jaafar El Fassi El Fihry High School (Casablanca, Morocco). His research focuses on numerical modeling of structures.

Mohammed Nassraoui was born in Beni Mellal, Morocco on November 26, 1973. He graduated in Mechanical Manufacturing from ENSET, Rabat, Morocco in 1996 and Doctorate degree in Mechanical Engineering from Hassan I University, Settat, Morocco. Currently, he is a Professor in Department of Mechanical Engineering at Higher School of Technology, Hassan II University, Casablanca, Morocco. His research interests focus on forming processes and advanced manufacturing modeling and design.

Otmane Bouksour was born in Rabat, Morocco, 1957. He received the Eng. degree in Civil Engineering from Mohammadia School of Engineers, University of Mohamed V (Rabat, Morocco) in 1981, and the M.Sc. and Ph.D. degrees in Structures and Mechanic of Solids from University of Sherbrooke (Quebec, Canada) in 1986 and 1990, respectively. Currently, he is a Professor in Mechanical Engineering Department at High School of Technology, University Hassan II of Casablanca (Casablanca, Morocco). His research interest is in industrial engineering, logistics and numerical modeling of structures.